LHCC Forward Physics and Diffraction, Instituto de Fisica Teorica, Madrid: Soft Diffraction and Total Cross section Chapter Summary

Valentina Avati, **Tim Martin**, Maciej Trzebinski, Ralf Ulrich, Orlando Villalobos-Baillie, *et. al.*.

CERN, **University of Warwick**, Polish Academy of Sciences, Karlsruher Institute of Technology, University of Birmingham.

22 April 2015

Introduction

- Chapter 3 of the yellow report focuses on the probability per inelastic interaction of generating one or more forward proton tags, either primary protons such as SD, elastic, or secondary protons. Phenomenological distributions are explored to gauge from MC interesting avenues of research based on these data. Measurements of the total, elastic and inelastic cross section are also covered.

Many thanks to our reviewers for their help in improving the flow and physics message of the chapter!

- Proton tag % and central vertex correlation.
- Forward proton mechanisms.
- Sensitive variables & methods.
- Elastic, inelastic & total cross section.

Proton Tag Probabilities

- Proton tag probability evaluated for the Pythia 8 MBR model with extrapolation to AFLA & AFP with `FPTrack`. Expect similar for CMS+TOTEM.
- Beam size is optics dependent - hence nominal distances are denoted for different β^* values.
- *Large theory + phenomenological modelling uncertainty.*

Single Proton Tag Probabilities

For Single Tag. **elastic** falls quickly for AFP (and is un-reconstructible), tag rate of 1–2% primarily SD events, some DD at higher ξ.

For ALFA/TOTEM vertical acceptance: elastics dominate at high β^*

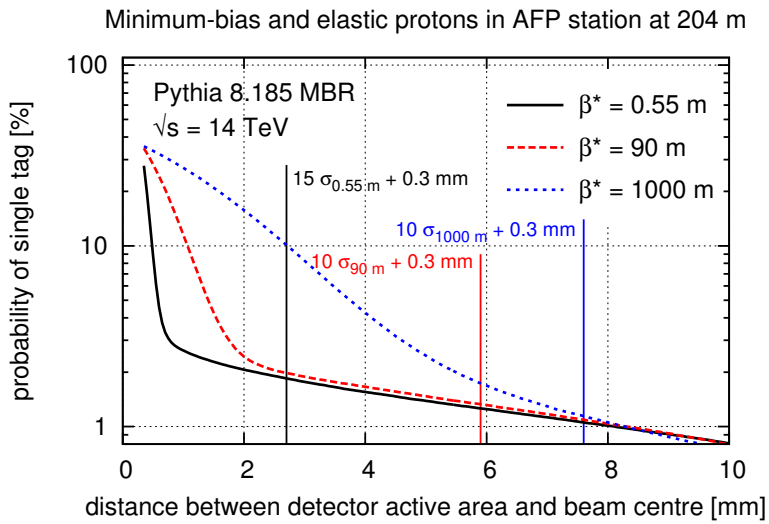

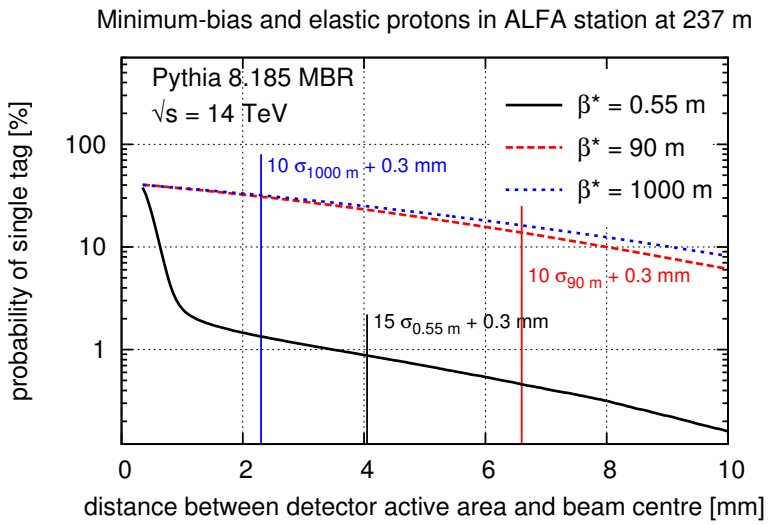

Double Proton Tag Probabilities

For double-tag in AFP/CT-PPS, **central diffraction** is the dominant factor at low β^*. ALFA/TOTM again dominated by elastic for high β^*

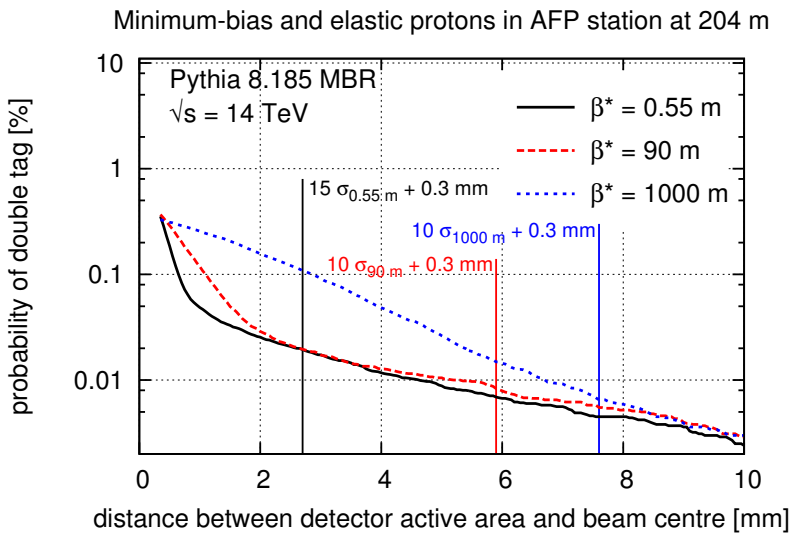

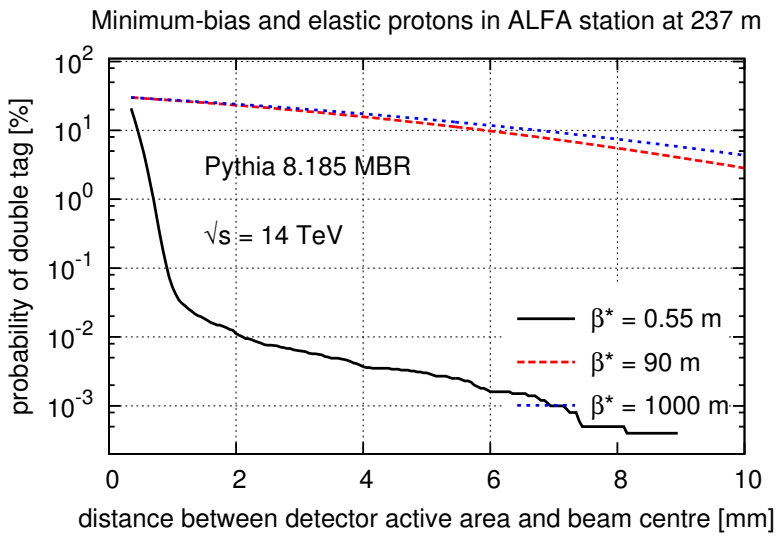

Central Vertex Correlation - Single Tag

- Given tag: Calculate subsequent central vertex probability for $n_{ch} \geq 4$ within $|\eta| < 2.5$ with a 50% chance to accept $100 < p_T < 500$ and 90% for $p_T > 500$.
- AFP/CT-PPS probability around 70% for nominal, 10% lower for high β^*
- For ALFA/TOTEM high β^*, probability is understandably small due to elastic scatters.

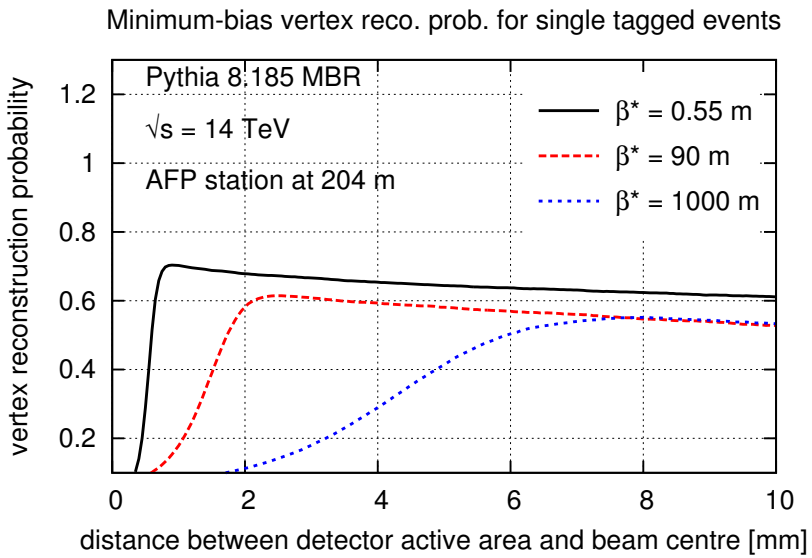

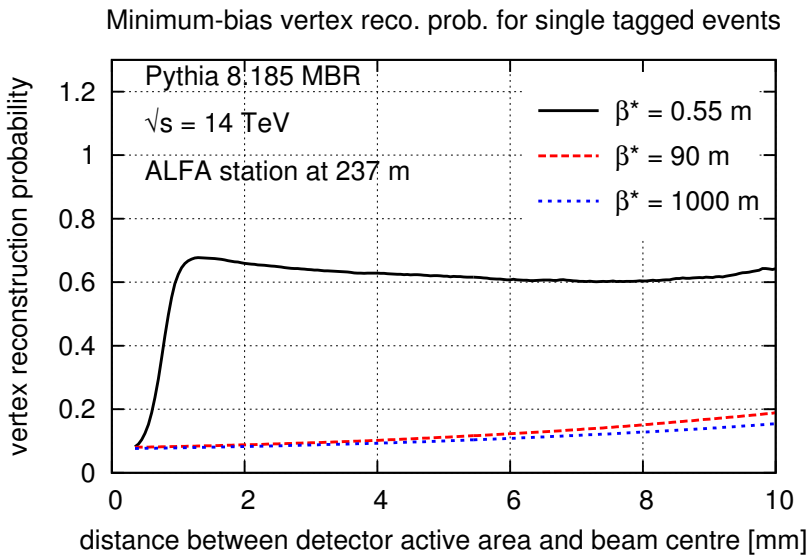

Single Tag Probabilities (nominal distance) for more MCs

- Single tag probabilities are shown also for different MC models, including a breakdown of Pythia (here Pythia 8 is `Tune A2 MSTW2008LO`) into its components.

	Cross Section $\sqrt{s} = 14$ TeV (mb)	AFP Tag Prob. $\beta^* = 0.55$ m (%)	ALFA Tag Prob. $\beta^* = 90$ m (%)	ALFA Tag Prob. $\beta^* = 0.55$ m (%)
`Herwig++` UE-EE-4	78.0	0.7	0.3	0.2
`EPOS` LHC	80.1	4.6	1.7	1.1
`Pythia 8` A2	79.3	2.5	0.8	0.6
`Pythia 8` A2 SD	12.9 (16%)	11.5	3.9	2.7
`Pythia 8` A2 DD	8.9 (11%)	3.3	0.6	0.8
`Pythia 8` A2 ND	57.5 (73%)	0.4	0.2	0.1

Diffractive System Correlations

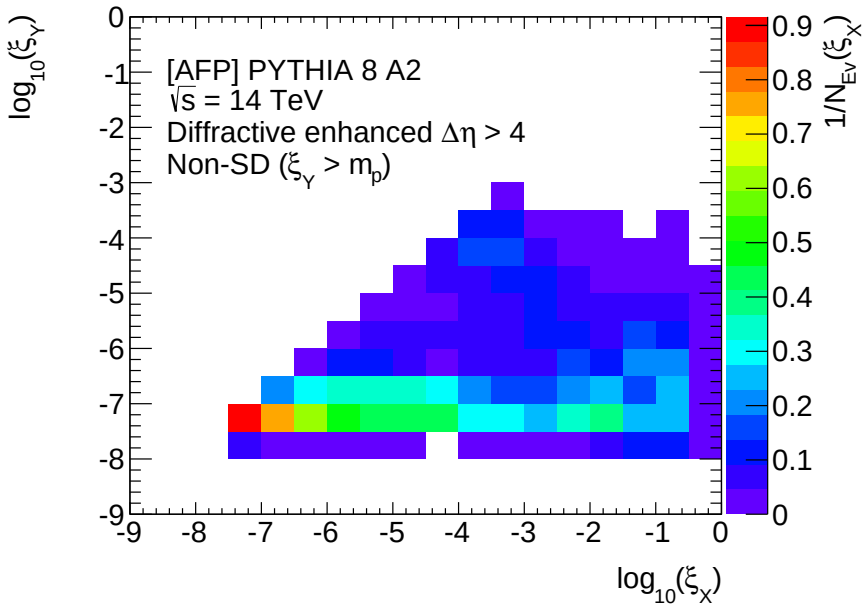

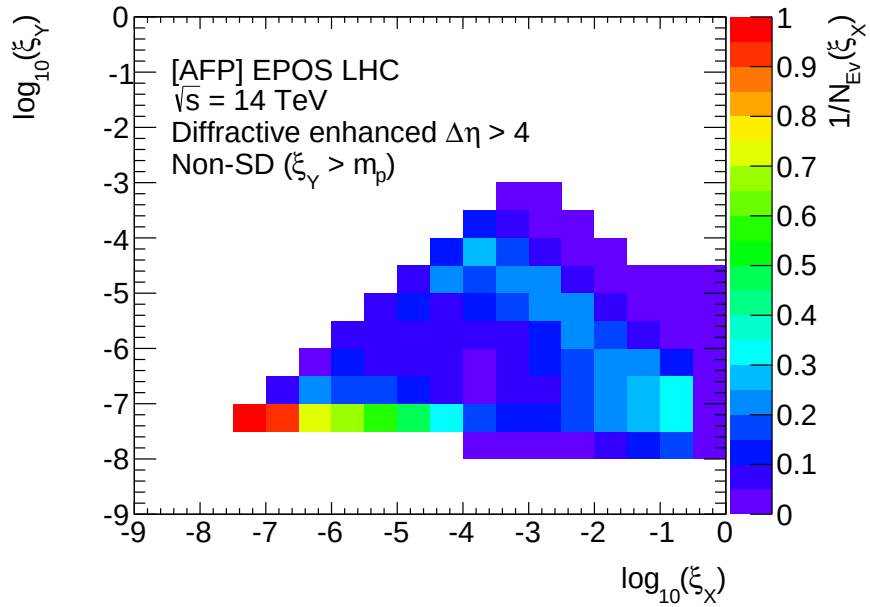

- The ability of Pythia to conserve the beam baryon number in a forward proton with reduced p is demonstrated in the kinematic plot of $\xi_{X,Y} = M_{X,Y}/s$ for the larger (X) and smaller (Y) systems.
- Observed as distinct lack of correlation between the two systems when $\sqrt{\xi_Y s} \sim M_p$.
- EPOS uses independent remnant scheme, displays anti-correlation at higher M_X.

Correcting to Diffractive σ

- In run 1, ALICE used their large trigger acceptance to select high purity SD and DD samples. These were then extrapolated to a fuller phase space.
- In run 2, ALICE, CMS and LHCb have additional forward shower scintillator counters - allowing access to even lower masses. In CMS, for example, up to $|\eta| < 9$.

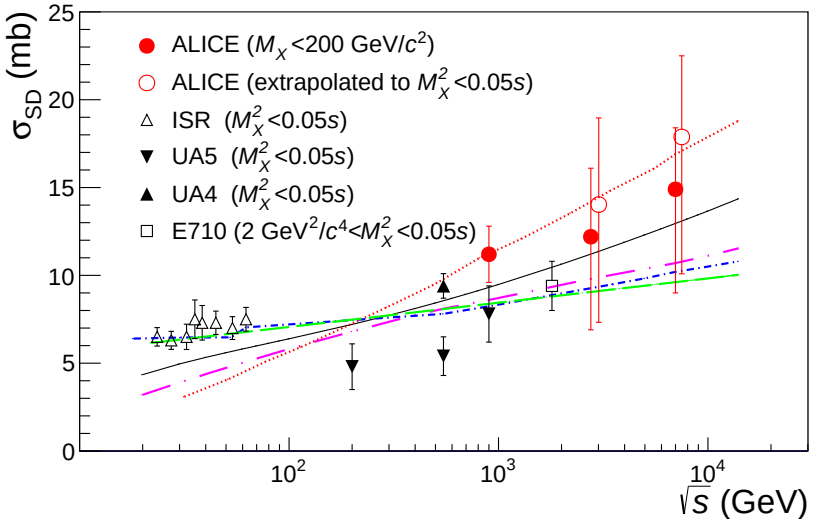

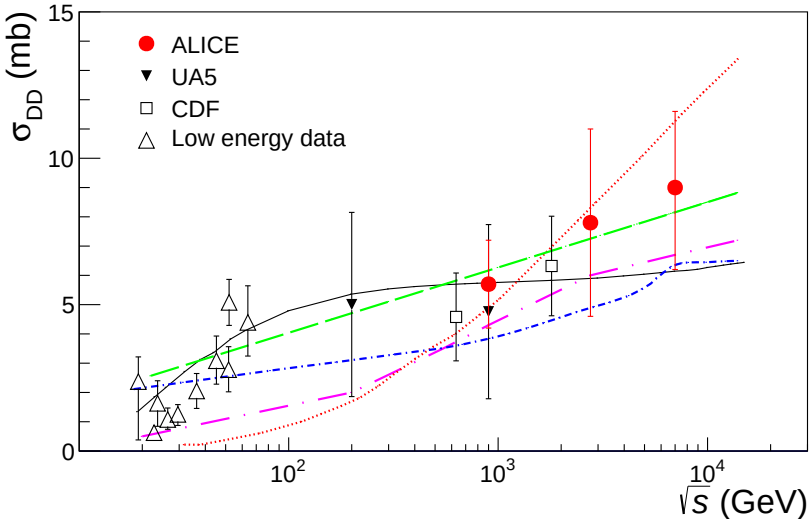

TOTEM Low Mass Double Diffraction

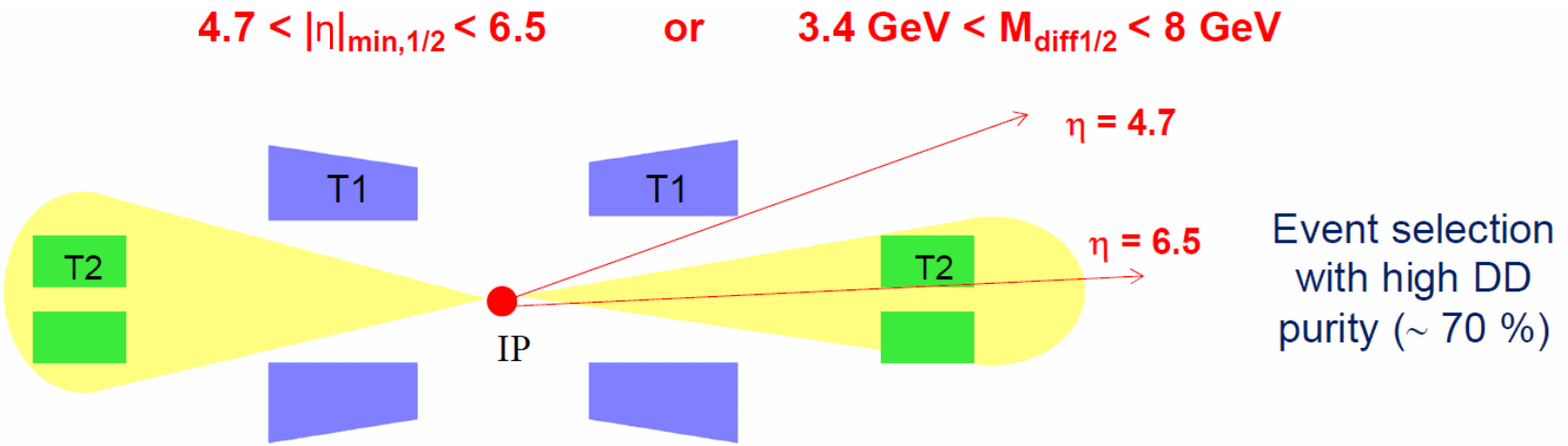

- Through using T1 and T2 as veto detectors, TOTEM have made valuable measure of low mass diffraction. $\sigma_{\mathrm{DD}} = 116 \pm 25 \mu$b for both diffractive systems $4.7 < |\eta_{\mathrm{min}} < 6.5$.
- Expect similar performance of extrapolation of σ_{tot} from $\beta^* = 90$ m data at $\sqrt{s} = 13$ TeV. Higher ($\beta^* = 2500$ m) optics foreseen to access Coulomb interference region.

Forward Rapidity Gap Spectrum

- For SD and low mass DD (where all M_Y particles are at $|\eta| > 5$. The diffractive cross section is investigated by reconstructing the largest rapidity gap from either edge of the detector at $\eta = \pm 5$.
- Can be compared to theoretical work from KMR arXiv:1402.2778 / 410.3261 / 1102.2844 to use all available data to form a model which globally describes LHC elastic and inelastic data.

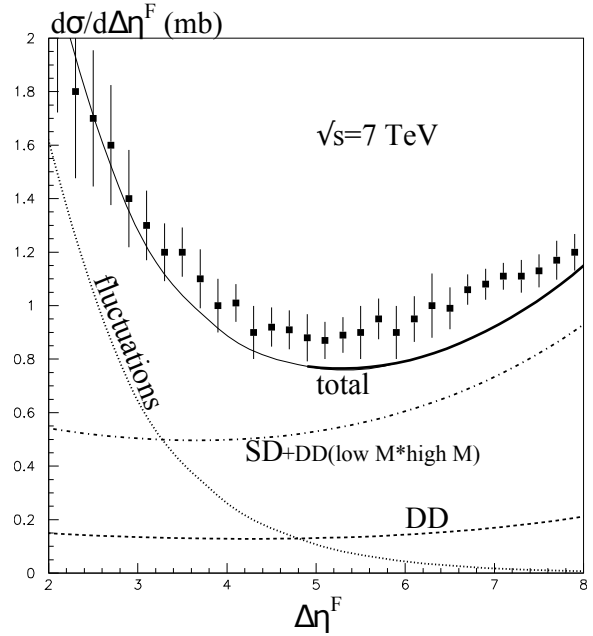

Rapidity gaps with p tag: Pythia

- For low β^*, AFP:
  - Single diffractive dominates at small gaps from high-mass SD interactions.
  - Tail of double diffractive events. Gap from larger system, tag from small (e.g. two body) dissociation.
- For high β^*, ALFA:
  - Overall smaller cross section. Low M_X SD at small t dominant in tail.
- *Both cases: the non-diff. bulk of σ_{tot} is strongly suppressed.*

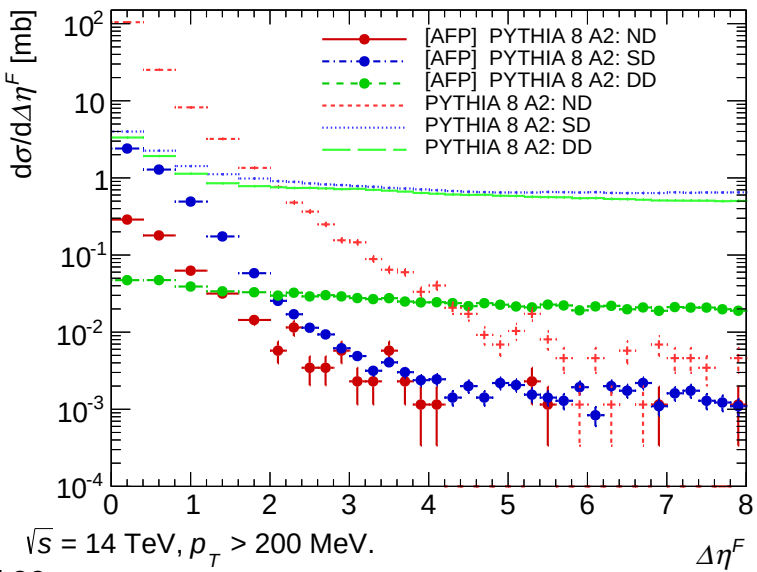

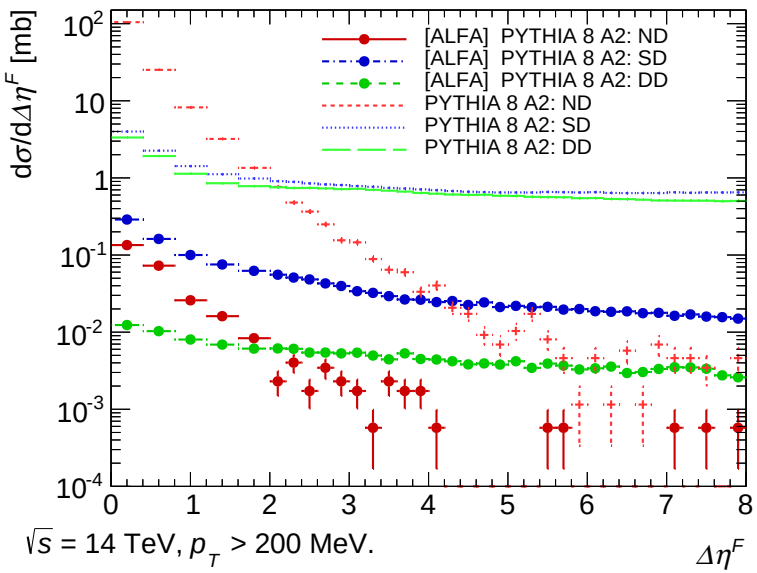

Rapidity gaps with p tag: Other Generators

- Model differences are greatly enhanced by the requirement of the forward proton tag.

All three generators considered predict a tail, the shape and transition from small to large gaps with and without a p tag will yield important information on modelling fragmentation and hadronisation in diffractive systems.

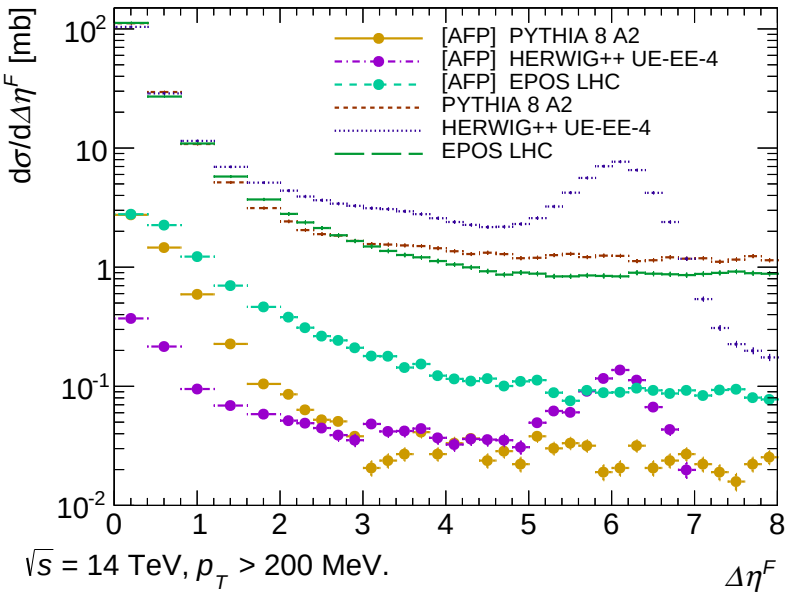

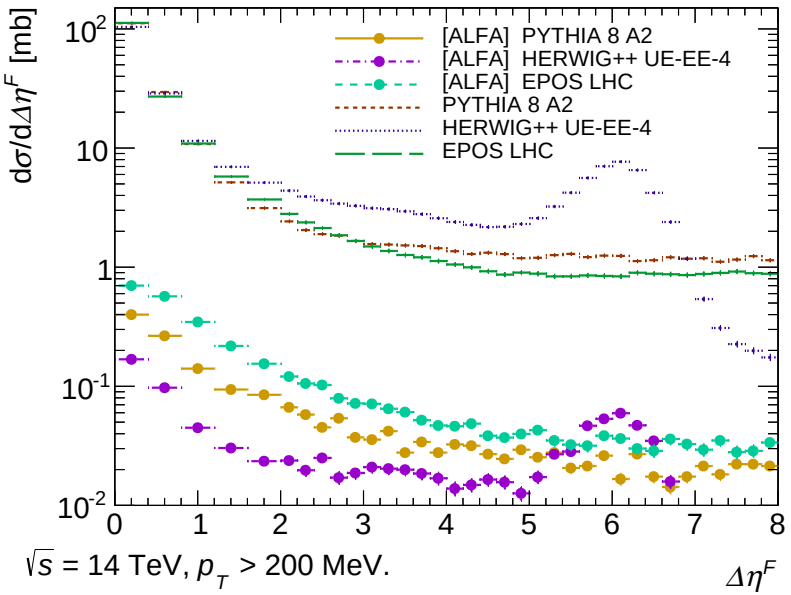

Rapidity Gaps as a probe of Hadronisation

- The importance of varying the p_T cut which defines the gap was illustrated in arXiv:1005.4839, a large dependence on the hadronisation (Lund string or cluster) is observed for small choices of p_T cut. (Top to bottom cuts of 1, 0.5 and 0.1 GeV on left.)

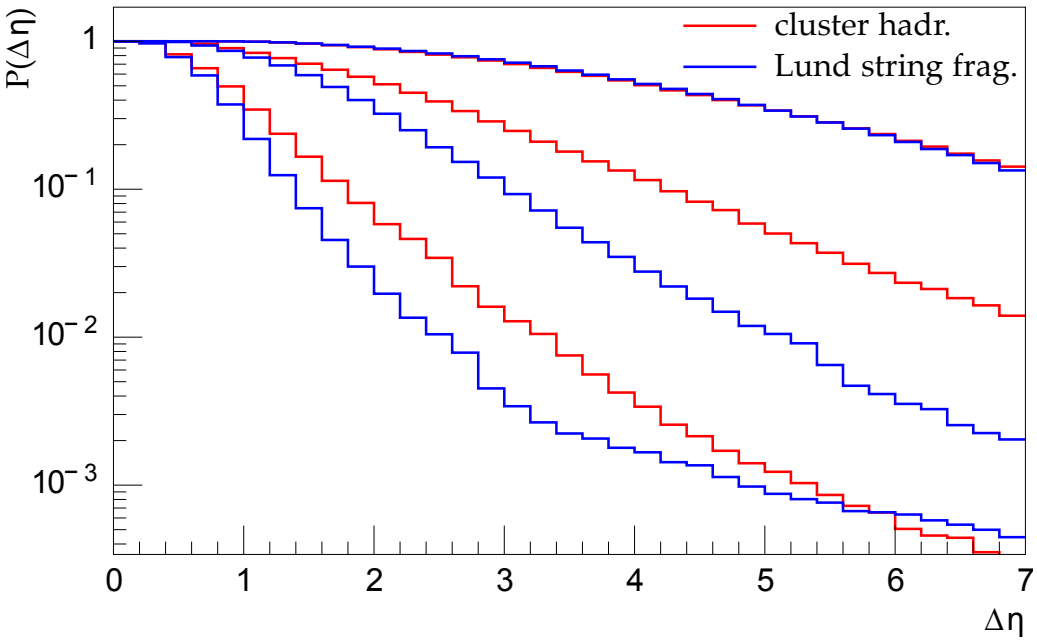

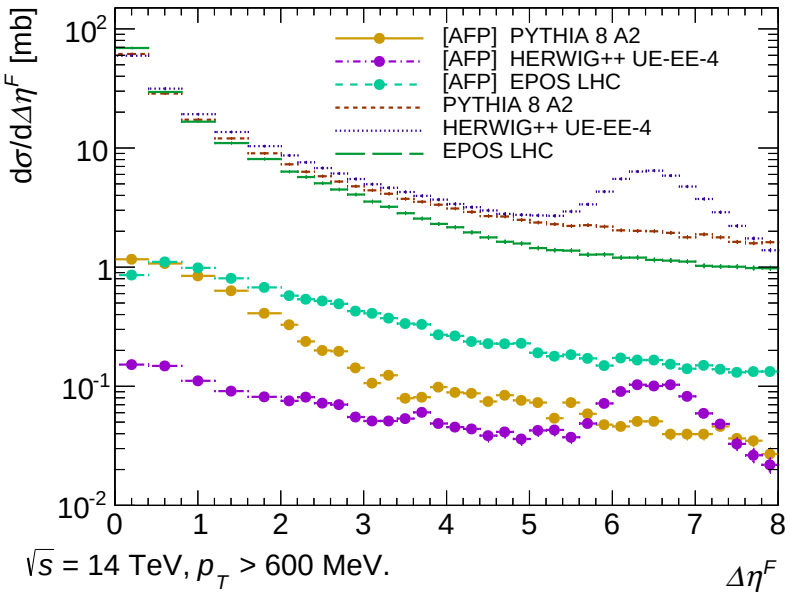

Extending Coverage with CASTOR

- The CASTOR calorimeter at CMS extends the coverage to $\eta = -6.6$. Wit no η segmentation, it acts to detect low mass systems in its acceptance.
- Good sensitivity (RMS noise $\sim$ 100–300 MeV/cell).
- Such data is complimentary to that collected by TOTEM's T2 telescope.

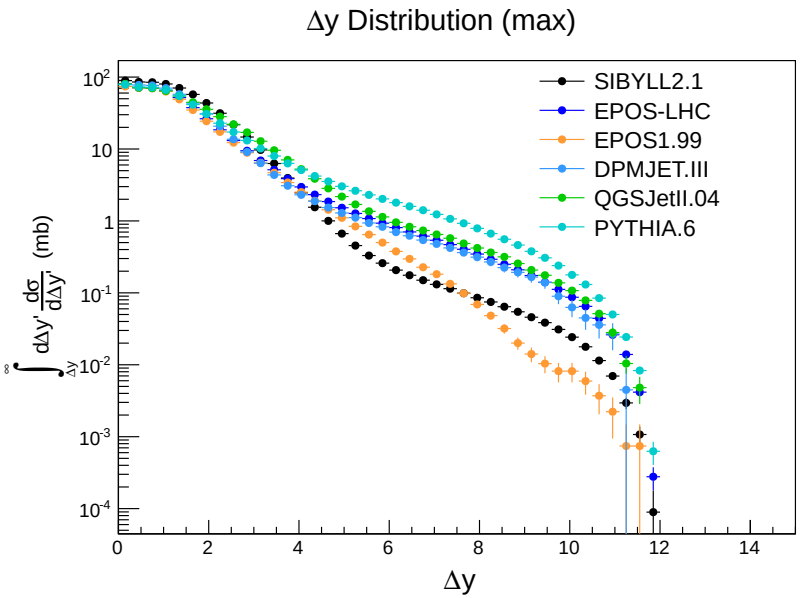

Total Inelastic Cross Section

- The inelastic cross section is measured within the acceptance of ALICE, ATLAS, CMS, LHCb and TOTEM (T1+T2). These measurements may then be extrapolated to the total cross section.

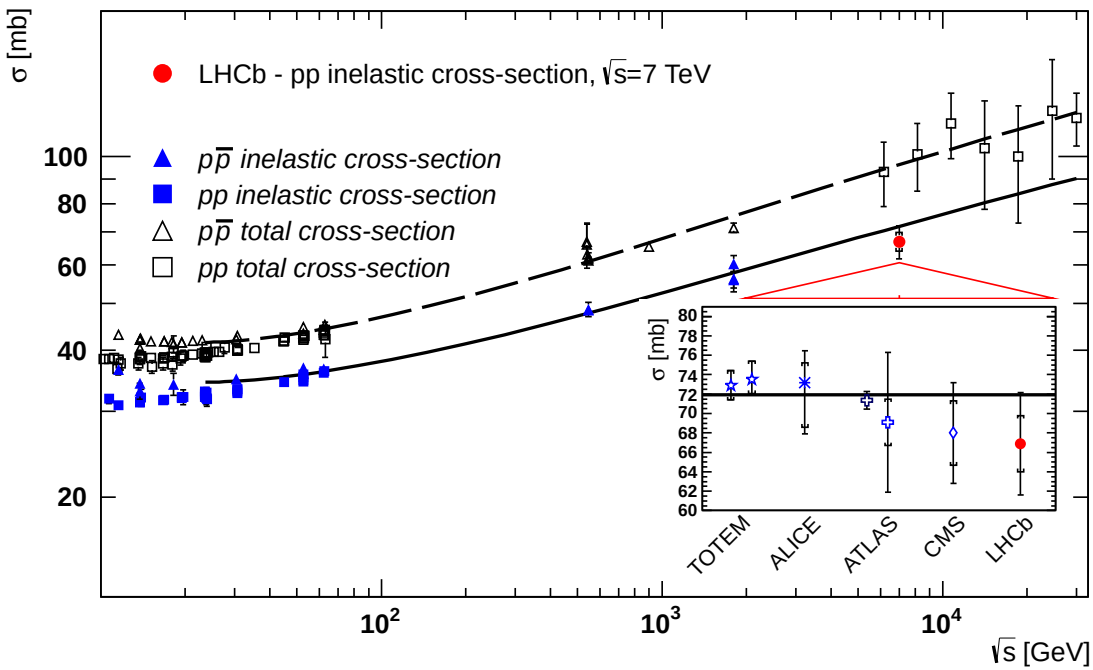

Total Cross Section: TOTEM and ALFA

- TOTEM has measured the total cross section and its breakdowns $\sigma_{\text{tot}}, \sigma_{\text{inel}}, \sigma_{\text{el}}$ and the slope of the elastic cross section $(d\sigma/d|t|)_{el} \propto e^{-Bt}$ (for small $|t|$) at 7 and 8 TeV and for different optics. ALFA has measured the total and breakdowns and the slope for 7 TeV with 90m optics.
- The total cross section is extracted from this slope via the optical theorem (other methods are available).
  - $\sigma_{\text{tot}}^2 = \frac{16\pi}{1+\rho^2} \frac{1}{\mathcal{L}} \frac{\mathrm{d}N_{\text{el}}}{\mathrm{d}t}\Big|_{t=0}$

At $\sqrt{s} = 13$ TeV, the acceptance limit $|t|_{\text{min,13TeV}} \approx 2|t|_{\text{min,7TeV}}$. Still good for extrapolation to $|t| \to 0$, but not for Coulomb interference region. Higher $\beta^* = 1$–2.5 km runs are foreseen to access this very low momentum exchange regime.

$-t$ Spectrum: TOTEM and ALFA

- Distribution of the differential elastic pp cross section by TOTEM and ALFA.
- ALFA highlight the region of high acceptance used to fit the nuclear B slope.
- TOTEM extend to higher $-t$ and show the diffractive minimum.

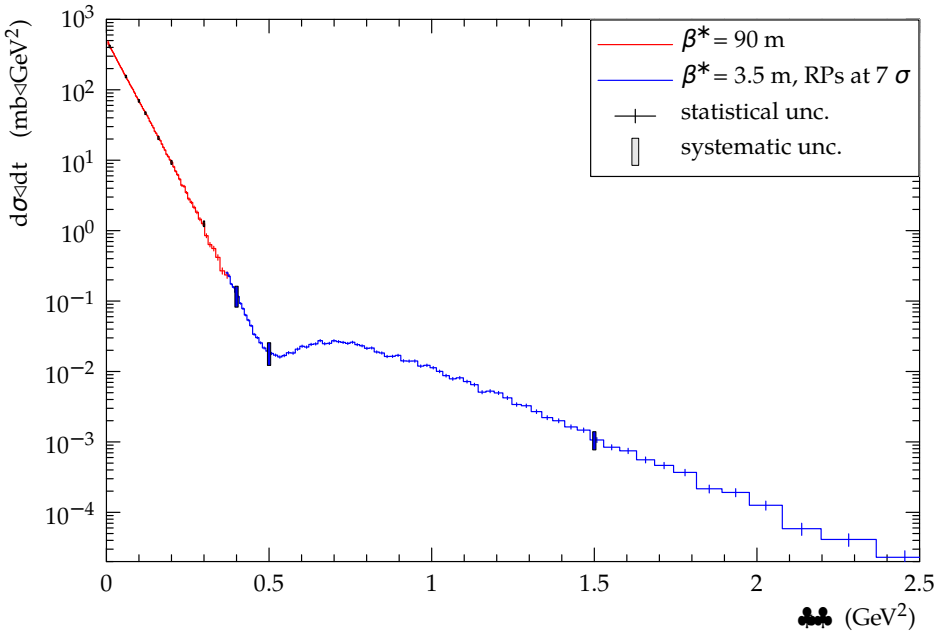

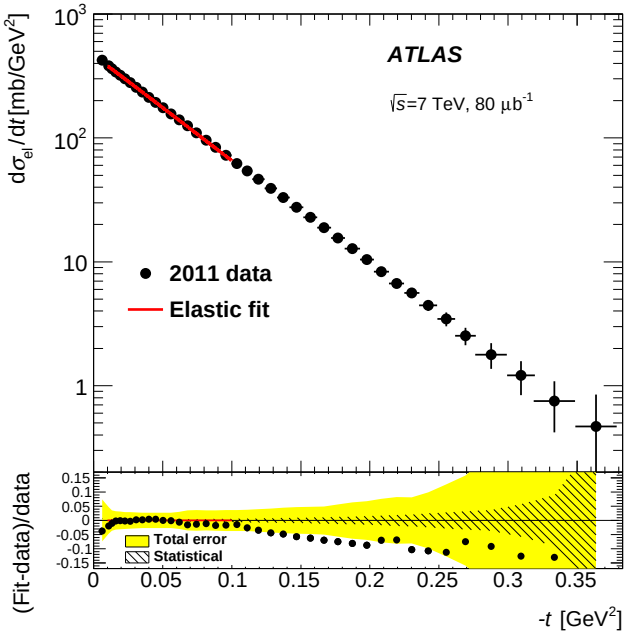

Total Cross Section: TOTEM and ALFA

- Fits to the total cross section by both collaborations, showing different TOTEM methodologies.
- ALFA uncertainty dominated by beam energy and luminosity uncertainty. Much work was done in minimising this.

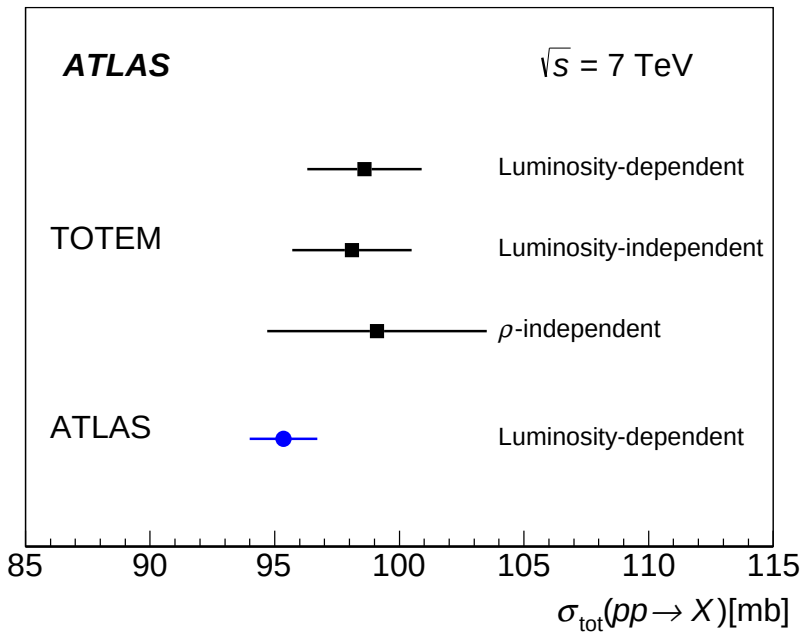

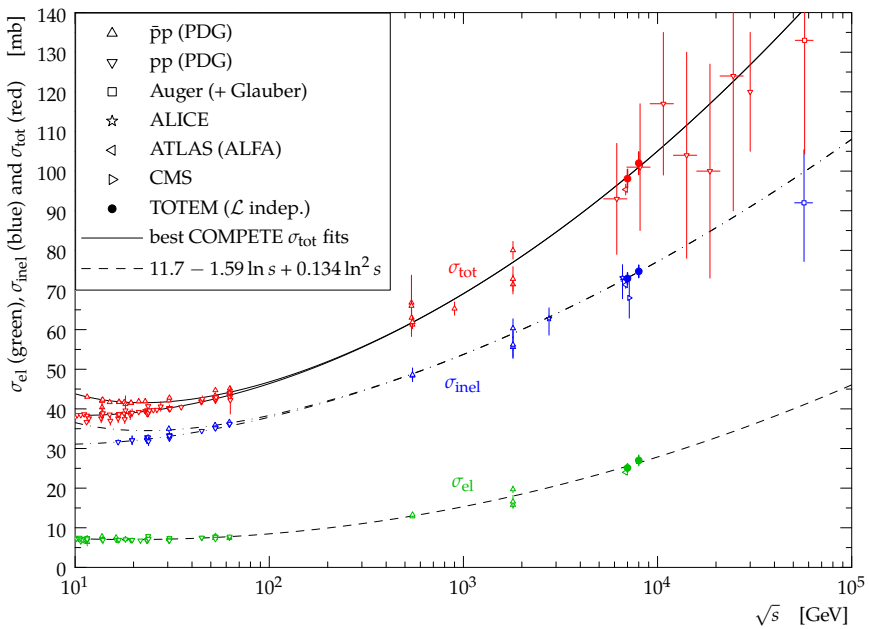

END OF CHAPTER 3 SUMMARY

Will now take a few moments to highlight some recent new soft physics results from ATLAS.

Bose Einstein Correlations [arXiv:1502.07947]

- BEC effects predict enhanced production of identical bosons.
- Correlation studies can probe the space-time geometry of the hadronisation region.
- This will materialise as an enhancement of a two-particle correlation function for same signed bosons at low $Q^2 = -(p_1 - p_2)^2$
  - ρ is 2-particle density fn, ρ_0 *excludes* BEC effects. p is 4-mom.
- Functional form can be described by the C_2 correlator $C_2(Q) = \frac{\rho(Q)}{\rho_0(Q)} = C_0[1 + \lambda e^{-QR}](1 + \epsilon Q)$
  - λ is coherence: 1=coherent, 0=incoherent(chaotic). QR dep. is from Fourier transform of space-time points. ϵ accounts for long-distance correlations not removed from ρ_0, C_0 is normalisation.

Bose Einstein Correlations [arXiv:1502.07947]

- Choice of reference sample is important. Needs to cancel out all two-particle correlations *not* due to the BEC effect.

Can mix tracks between hemispheres or events, however $\rho_0(Q)$ should include all relevant momentum correlations, from both the local and global conservation laws.

Can use unlike sign pairs. However resonances can mimic BEC effects.

- In ATLAS we use an unlike sign reference taken in double-ratio with MC to cancel out resonant production.
- This works well, only the ρ meson is not fully accounted for, this region is excluded from fits.

Bose Einstein Correlations [arXiv:1502.07947]

- $R_2(Q) = \frac{C_2 Q}{C_2^{\mathrm{MC}}} = \frac{\rho(\mathrm{likesign})/\rho(\mathrm{unlikesign})}{\rho^{\mathrm{MC}}(\mathrm{likesign})/\rho^{\mathrm{MC}}(\mathrm{unlikesign})}$

Note: MC does not simulate the BEC effect, data additionally corrected for Couloumb effects.

Enhancement of correlations clearly observed at low Q

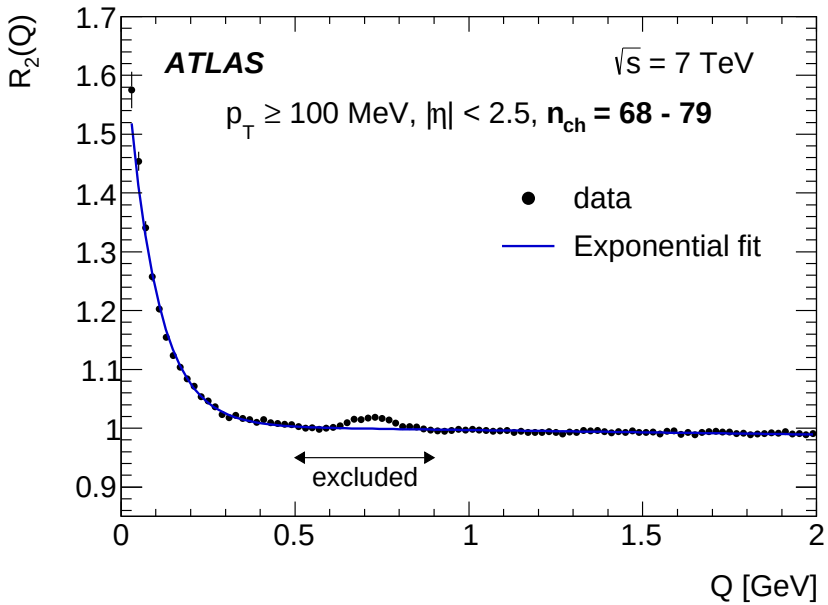

Bose Einstein Correlations: N_{Ch} Dep.

- Dependence on the coherence decreases faster with multiplicity at 900 GeV than at 7 TeV, may be well fitted to an exponential fn.
- The size parameter follows a cubic expansion up until around $N_{Ch} = 50$, after which we observe *for the first time a saturation of the effective source radius.*
- These data taken with dedicated high multiplicity trigger. CMS comparison is mixed-event reference, double ratio.

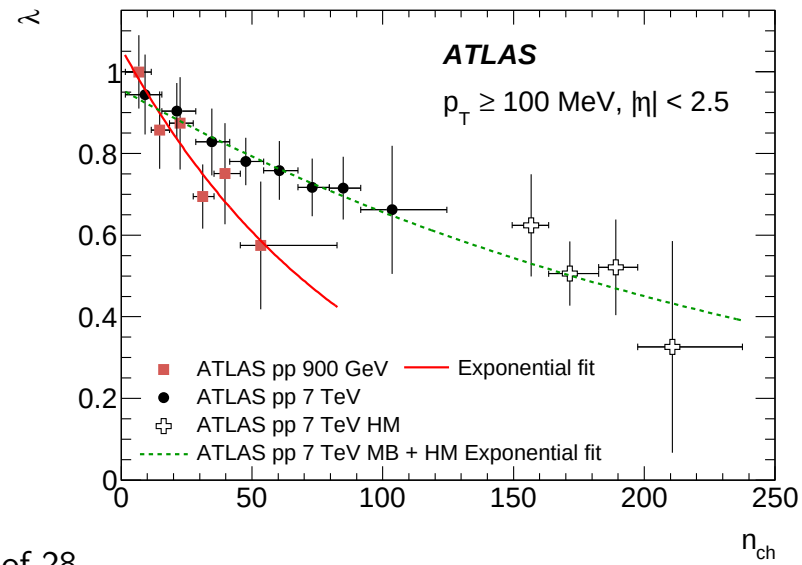

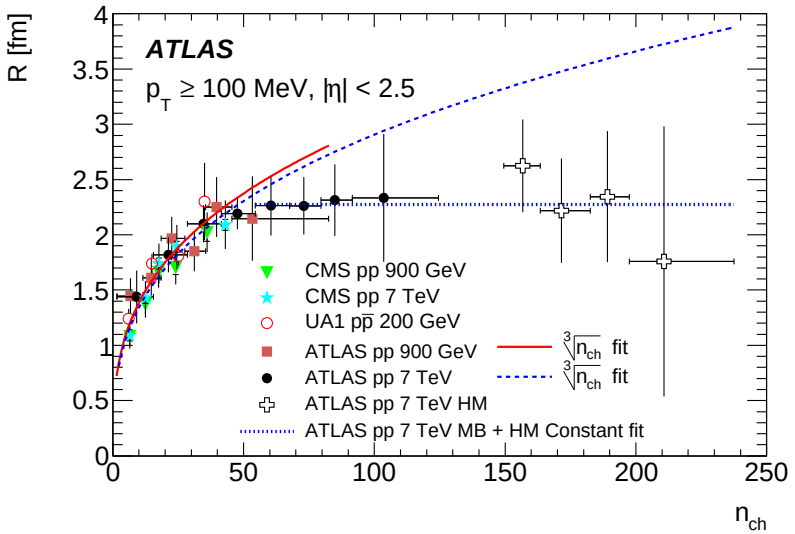

Bose Einstein Correlations: k_T Dep.

- Dependence plotted as a function of the average transverse pair momentum $k_T = |p_{T,1} + p_{T,2}|/2$
- Decrease in λ and R both modelled well by an exponential, including at high multiplicities.
- STAR & E735 used mixed-event reference, Gaussian fit (here multiplied by $\sqrt{\pi}$), single ratio.

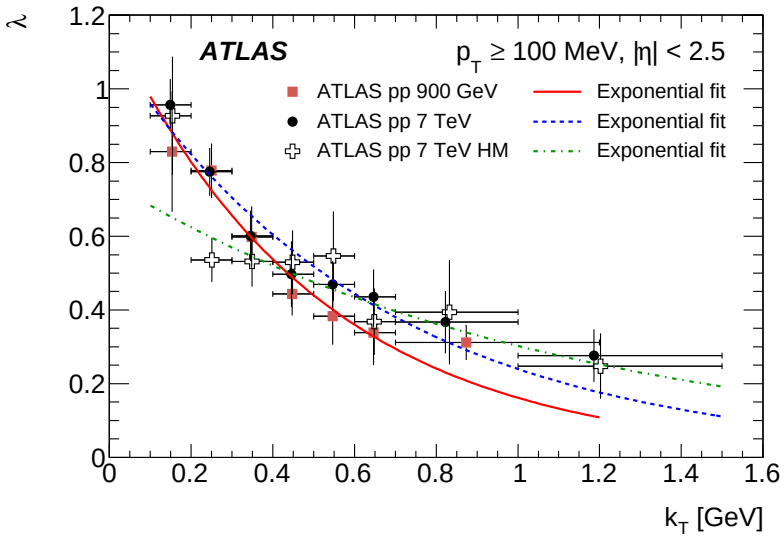

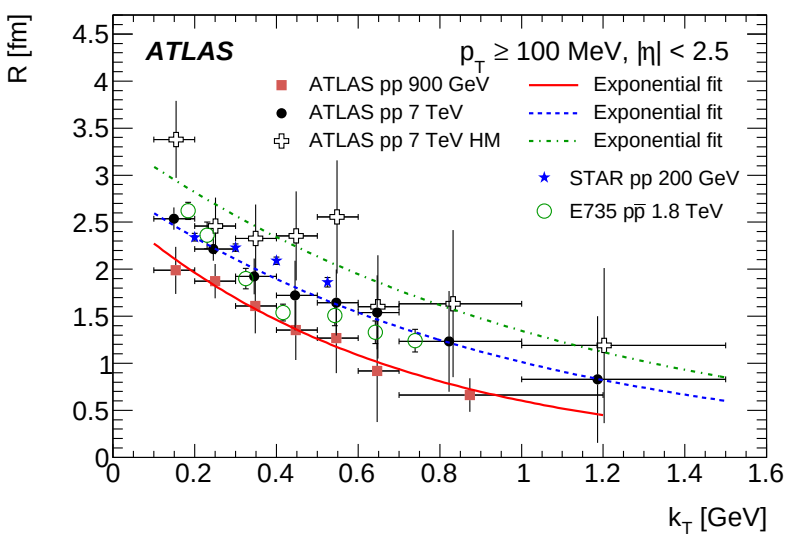

Transverse Polarisation of Λ and $\bar{\Lambda}$ arXiv:1412.1692 [hep-ex]

- Strongly produced spin $\frac{1}{2}$ Λ and $\bar{\Lambda}$ can have no polarisation parallel to the Λ momentum vector (parity conservation).
- Large values of Λ polarisation are inconsistent with pQCD. Soft models can explain some individual hyperons but none of yet all hyperons.

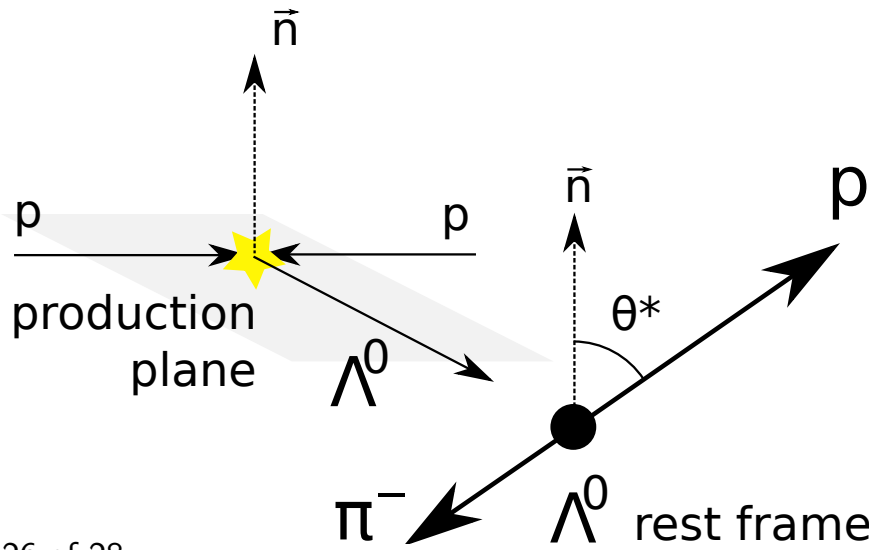

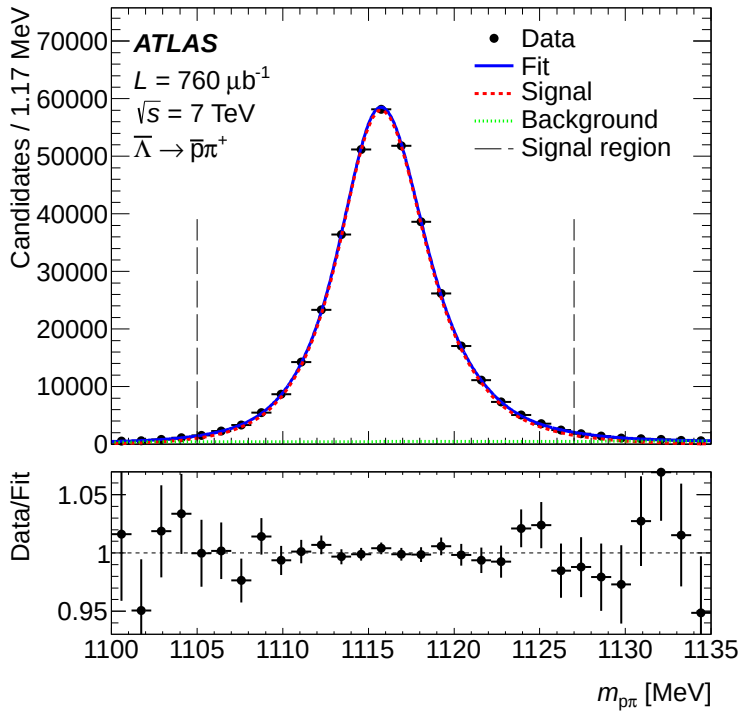

Transverse Polarisation of Λ and $\bar{\Lambda}$ arXiv:1412.1692 [hep-ex]

- Past experiments have measured large (up to 30%) Λ transverse polarisation w.r.t. the production plane in p-p and p-Ion collisions.
- ATLAS measure the transverse polarisation differential in Feynman-x ($x_F = p_z/p_{\text{beam}}$) and p_T with respect to the beam line.
- Polarisation extracted from the angular distribution of Λ & $\bar{\Lambda}$ decay products via method of moments.
  - For any polarisation P, the first moment of the angular distribution may be written as a linear combination of the un-polarised $E(0)$ and fully-polarised $E(1)$ moments: $E(0) + [E(1) - E(0)]P$.

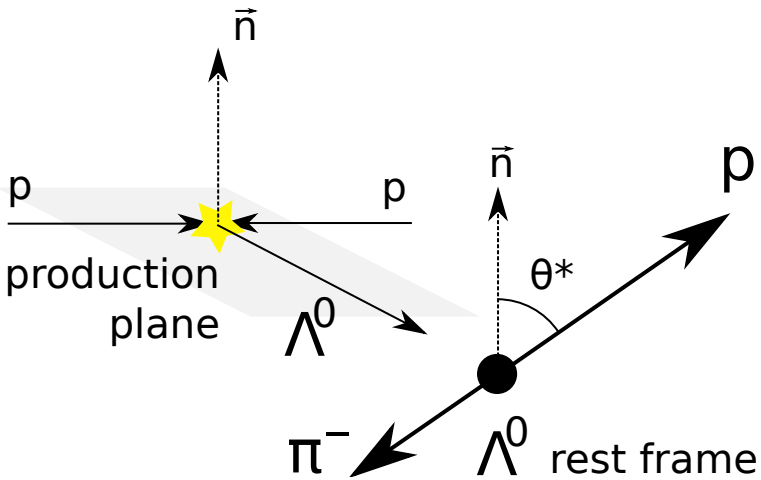

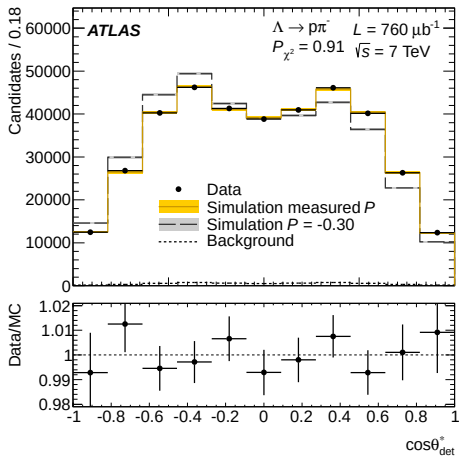

Transverse Polarisation of Λ and $\bar{\Lambda}$ arXiv:1412.1692 [hep-ex]

- Results, presented in the fiducial volume of $0.8 < p_{\mathrm{T}} < 15$ GeV, $5 \times 10^{-5} < x_{\mathrm{F}} < 0.01$ and $|\eta| < 2.5$

$$P_{\Lambda} = -0.010 \pm 0.005(\text{stat.}) \pm 0.004(\text{syst.})$$

  are compatible with zero polarisation. Equivalently for $P_{\bar{\Lambda}} = 0.002$.

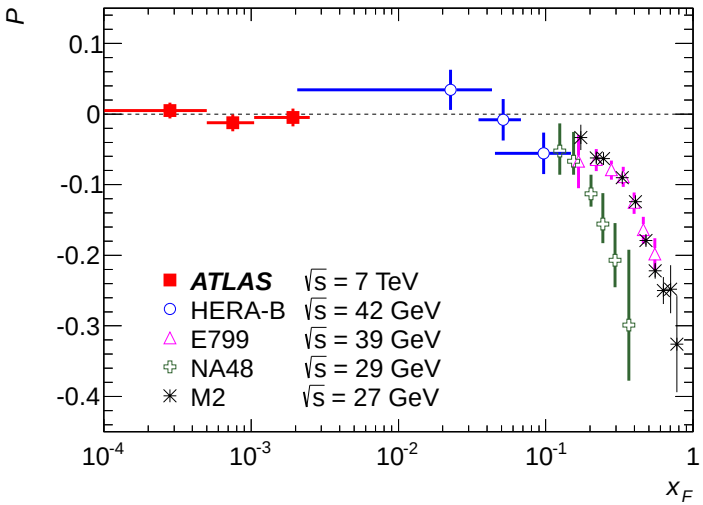

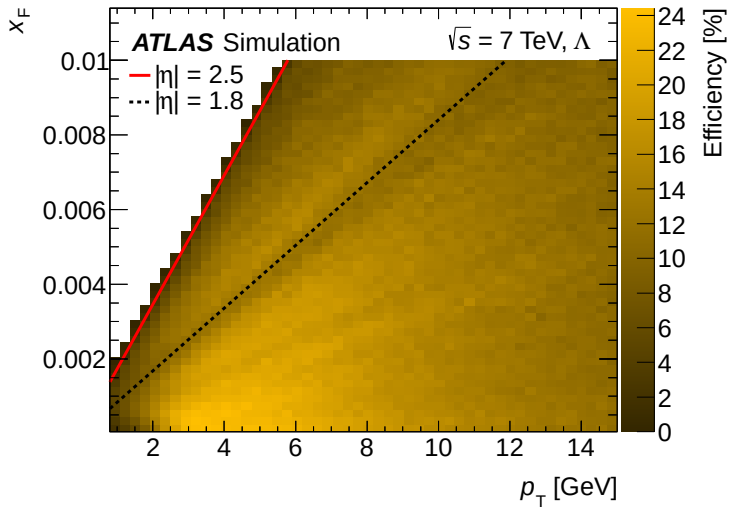

- Reconstruction efficiencies are provided as a function of p_{T} and x_{F} to allow model builders to weight their Λ baryons for comparison with ATLAS data.